Electronic Supplementary Material (ESI) for Nanoscale Horizons.

Supporting information

Colloidal Heterostructured Quantum Dots Sensitized Carbon Nanotubes-TiO_2 Hybrid Photoanode for High Efficiency Hydrogen Generation

Gurpreet Singh Selopal [a, b], Mahyar Mohammadnezhad [b], Fabiola Navarro-Pardo [a, b], François Vidal [b], Haiguang Zhao [c, *] Zhiming M. Wang[b*] and Federico Rosei [a,b,*]

[a]Institute of Fundamental and Frontier Sciences, University of Electronic Science and Technology of China, Chengdu 610054, People's Republic of China.

[b]Institut National de la Recherché Scientifique, Centre Énergie, Matériaux et Télécommunications, 1650 Boul. Lionel Boulet, J3X 1S2 Varennes, Québec, Canada.

[c]The Cultivation Base for State Key Laboratory & College of Physics, Qingdao University, No. 308 Ningxia Road, Qingdao 266071, PR China

Email : hgzhao@qdu.edu.cn ; zhmwang@uestc.edu.cn ; rosei@emt.inrs.ca

Experimental

Synthesis of CdSe QDs and core/shell QDs

CdSe QDs were synthesized using the hot-injection approach[1]. Deposition of CdS layers on CdSe QDs followed procedures described elsewhere[2]. Typically, in a 50-mL round-bottom flask, OLA (5 ml), ODE (5 mL) and CdSe QDs (~2×10^{-7} mol in hexane) were degassed at 110 °C for 30 min. The reaction flask was re-stored with N_2 and the temperature was further raised to 240 °C with stirring. The $Cd(OA)_2$ dispersed in ODE (0.25 mL, 0.2 M) was added dropwise and the mixture was allowed to react for 2.5 h, followed by dropwise addition of 0.2 M sulfur in ODE with the same volume. The shell was further annealed for 60 min. All subsequent shells were annealed at 240 °C for ~10 min following the injection of sulfur and ~2.5 h following dropwise addition of the $Cd(OA)_2$ in ODE. Sulfur/$Cd(OA)_2$ addition volumes for shell addition cycles 1-6 were as follows: 0.25, 0.36, 0.49, 0.63, 0.8, and 0.98 mL, respectively.

Graded alloyed shells were synthesized by tailoring the molar ratio of S:Se during *in situ* growth of each layer $CdSe_xS_{1-x}$ (x = 0.9~0.1) over the CdSe core QDs. Subsequently another two layers of CdS were coated on the alloyed shell. The reaction was cooled to room temperature using ice water. Ethanol was added, and then the suspension was centrifuged and the supernatant was removed. The QDs were then dispersed in toluene for further characterization.

Anode preparation

A thin and compact TiO_2 blocking layer was deposited on ultrasonically cleaned FTO glass substrates by hydrolysis of 0.50 mM $TiCl_4$ solution at 70 °C for 30 min. It was then annealed at 500 °C for 30 min under ambient atmosphere and left to cool down to room temperature.

A good dispersion of MWCNTs (an average length of 10 μm) in ethanol was prepared by mixing 6 mg of MWCNTs in 15 mL of ethanol and sonicated for 3 hours. TiO_2-MWCNTs hybrid pastes with different concentration of MWCNTs were prepared by mixing the precise amount of ethanolic suspension of MWCNTs into a known weight of TiO_2 paste composed of small (20 nm in diameter) and large (up to 450 nm in diameter) size anatase particles (18NR-AO). Subsequently, the above prepared TiO_2-MWCNTs hybrid pastes were deposited on top of the compact TiO_2 layer by tape casting. A drying process was followed for 15 min at ambient conditions and then placed on a hot plate for 6 min at 120 °C. A second layer was then deposited on the top, following the same procedure[3]. All the photoanodes were then annealed at 500 °C for 30 min under ambient conditions. For a systematic comparison, bare TiO_2 photoanodes were

also prepared under the same conditions. The thickness of all photoanodes was measured using a profilometer.

ZrO_2 film preparation

ZrO_2 films were prepared by using a commercial ZrO_2 nanopowder (Aldrich, particle size ＜100 nm). A single layer of ZrO_2 film was deposited on FTO glass by tape casting, then annealed in air at 500 °C for 30 min and cooled down to room temperature. We studied the electron transfer rate by using transient fluorescence spectroscopy on QDs deposited into TiO_2 or ZrO_2 mesoporous films. The ZrO_2/QDs film serves as a benchmark sample, in which the energy levels do not favour electron/hole transfer. The hole transfer rate in this experiment was monitored by immersing the ZrO_2/QDs film into the Na_2S/Na_2SO_3 solution (pH ~13) as a hole scavenger.

Results and Discussion

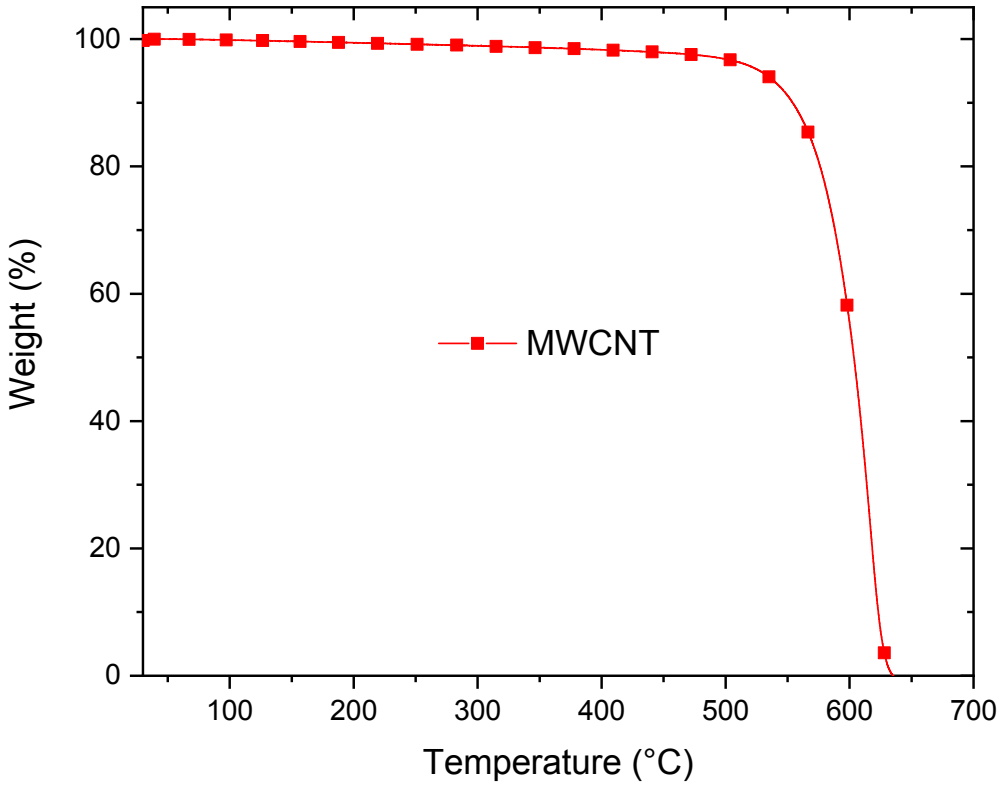

Figure 1S. Thermogravimetric analysis of MWCNTs powder.

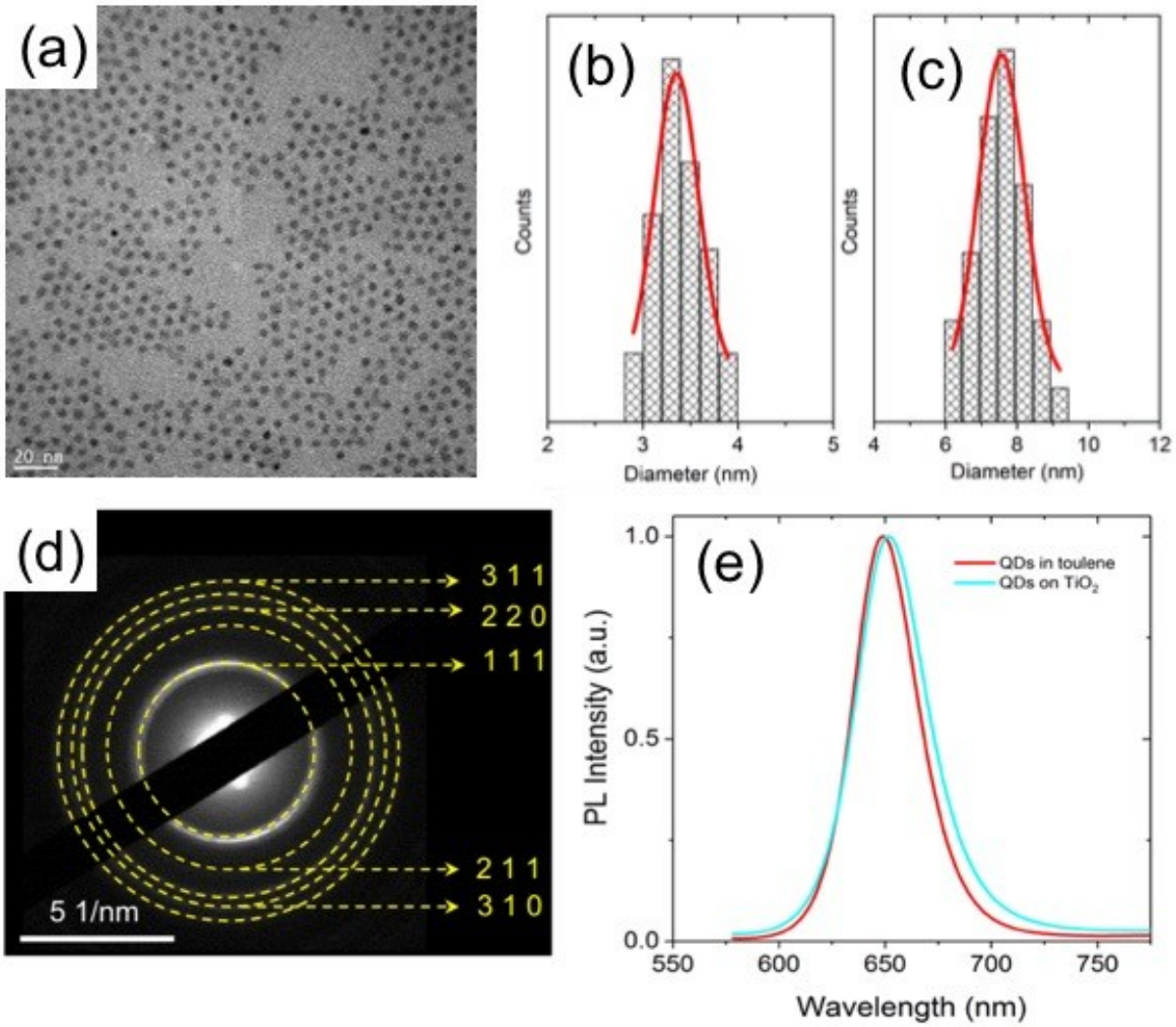

Figure 2S. Structural properties of colloidal QDs: (a) TEM image of as-synthesized CdSe core QDs before the growth of alloyed shell. Size distribution (solid lines are Gaussian fit of the experimental data): (b) CdSe core QDs; (c) gradient alloyed heterostructured CdSe/$(CdSe_xS_{1-x})_5$/$(CdS)_2$QDs; (d) Selected area electron diffraction pattern (SEAD) of gradient alloyed heterostructured CdSe/$(CdSe_xS_{1-x})_5$/$(CdS)_2$QDs. (e) PL spectra of as-synthesized gradient alloyed heterostructured CdSe/$(CdSe_xS_{1-x})_5$/$(CdS)_2$QDs in toluene and deposited on TiO_2 mesoporous film.

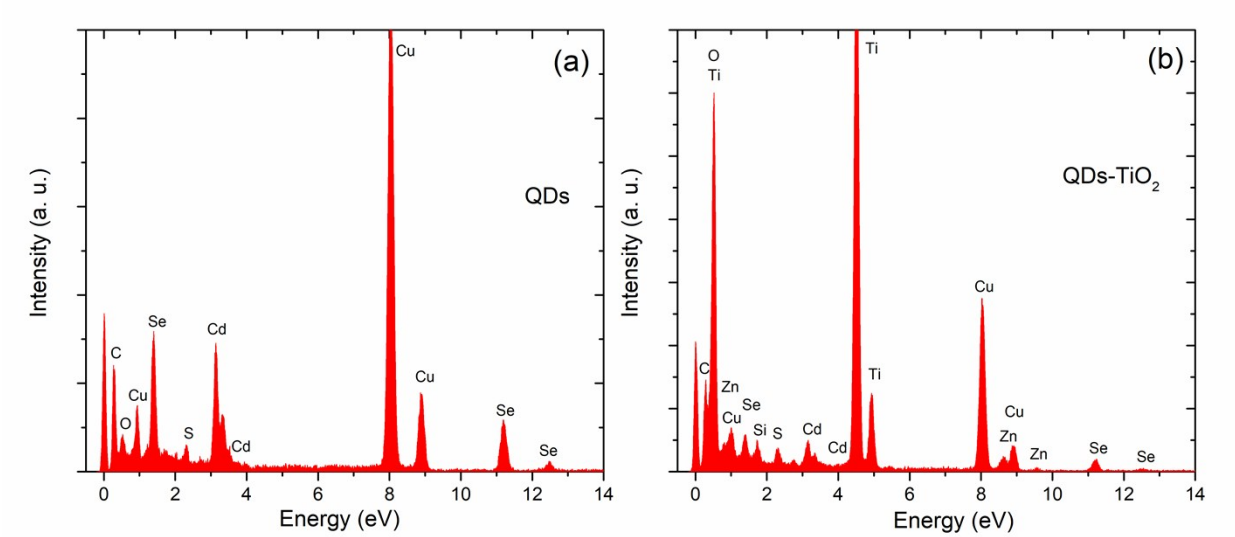

Figure 3S. EDS spectra of: (a) colloidal heterostructured QDs; (b) TiO_2/QDs/ZnS/SiO_2 mesoporous film.

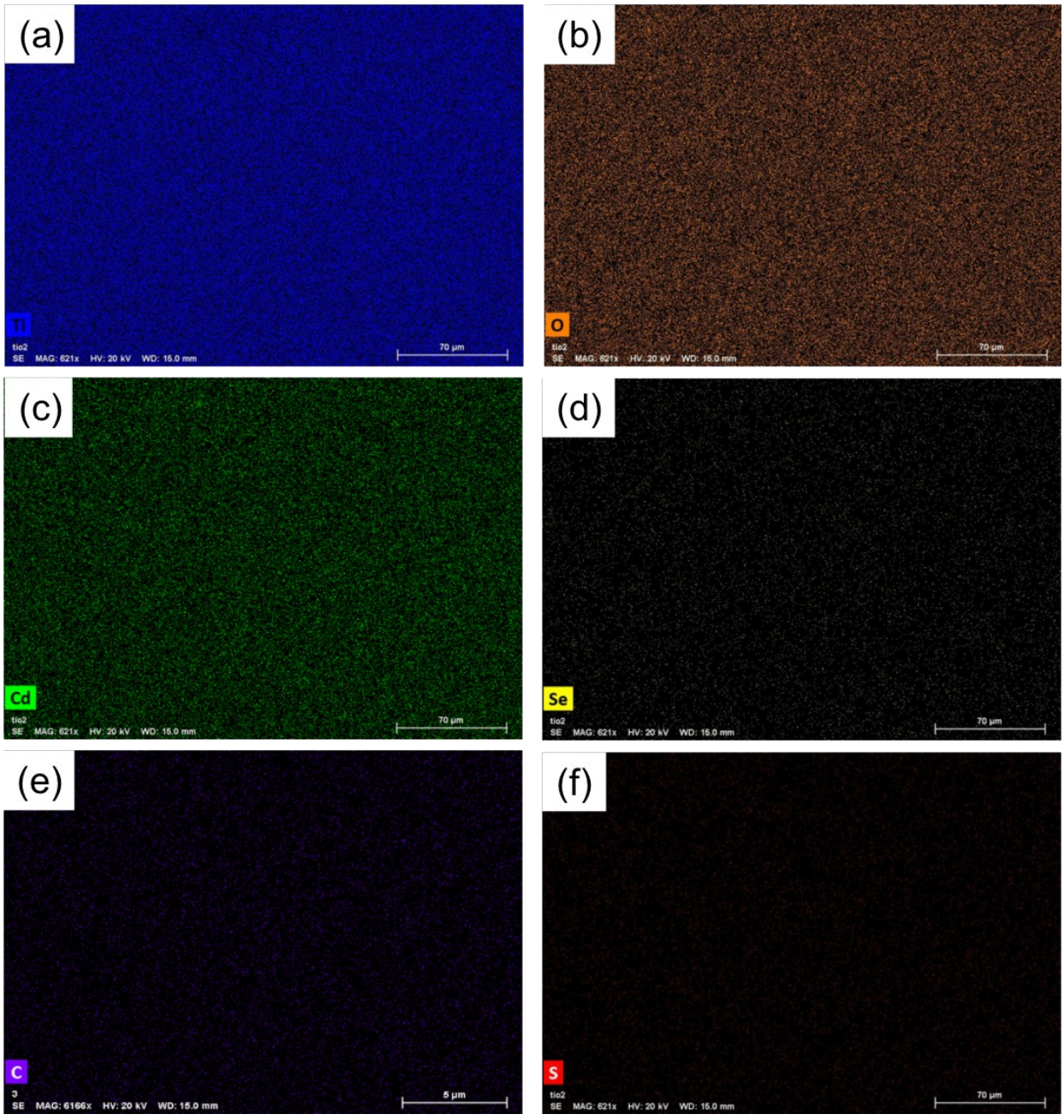

Figure 4S. Elemental mapping by EDS spectroscopy of TiO_2/QDs: (a) Ti; (b) O; (c) Cd; (d) Se; (e) C (f) and (f) S.

Table 1 S. The wt % of the different elements of colloidal QDs sensitized TiO_2 coated photoanode, according to EDS measurements.

Elements	Ti	O	Cd	Se	S	C
Wt. %	28.93	65.19	0.39	0.11	0.09	5.29

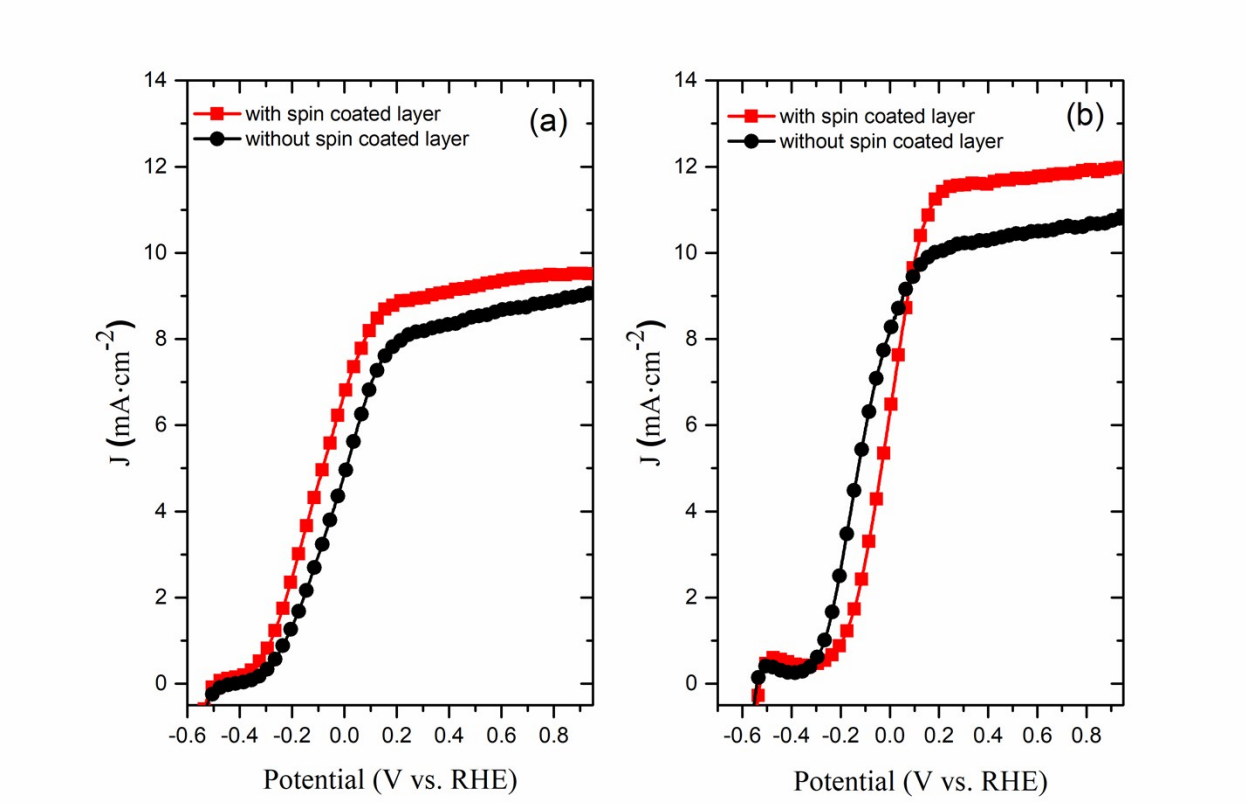

Figure 5S. Comparison of photocurrent density versus bias potential (versus RHE) of PEC systems based on colloidal heterostructured QDs sensitized photoanodes with (red square) and without (black circle) spin coated layer of 20 nm nanoparticles under one sun continuous illumination (AM 1.5 G, 100 mW.cm^{-2}): (a) pristine TiO_2/QDs; (b) TiO_2/QDs-MWCNTs hybrid photoanodes.

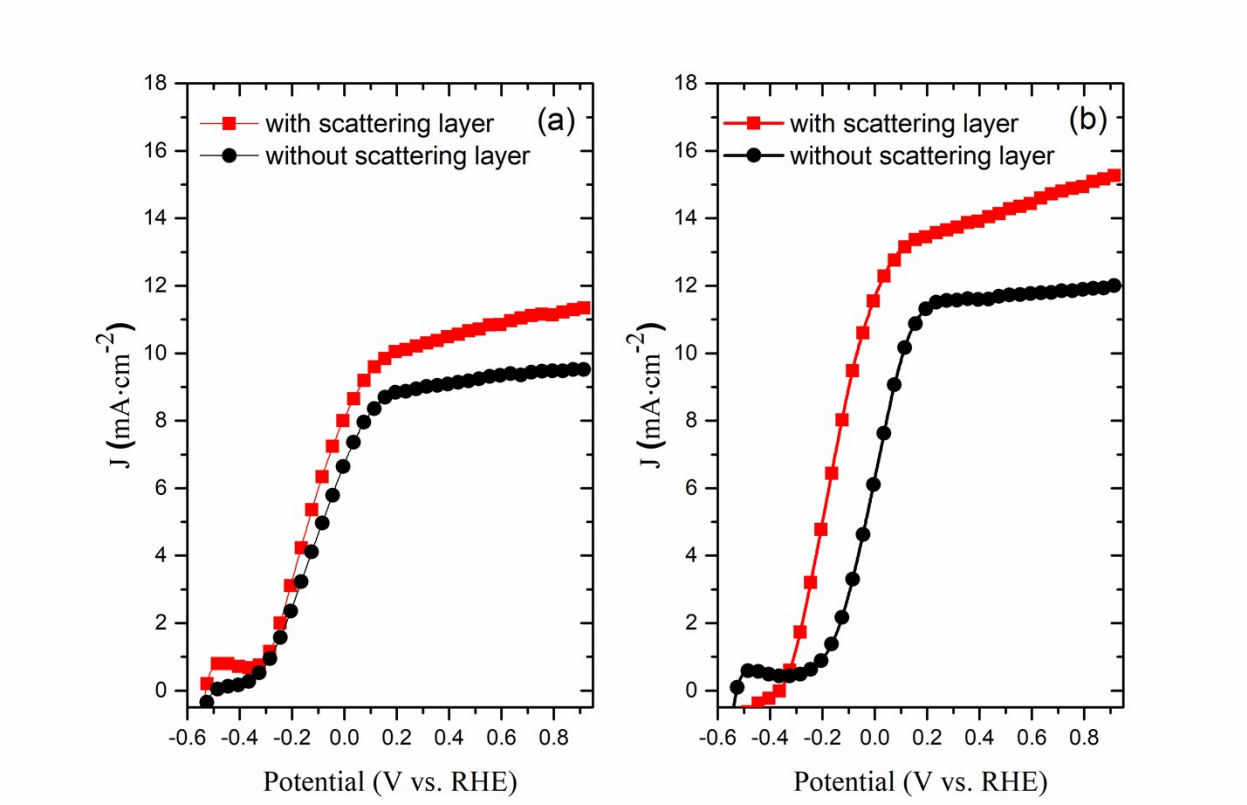

Figure 6S. Comparison of photocurrent density versus bias potential (versus RHE) of PEC systems based on colloidal heterostructured QDs sensitized photoanodes with (red square) and without (black circle) scattering layer of 150-400 nm nanoparticles under one sun continuous illumination (AM 1.5 G, 100 mW.cm^{-2}): (a) pristine TiO_2/QDs; (b) TiO_2/QDs-MWCNTs hybrid photoanodes.

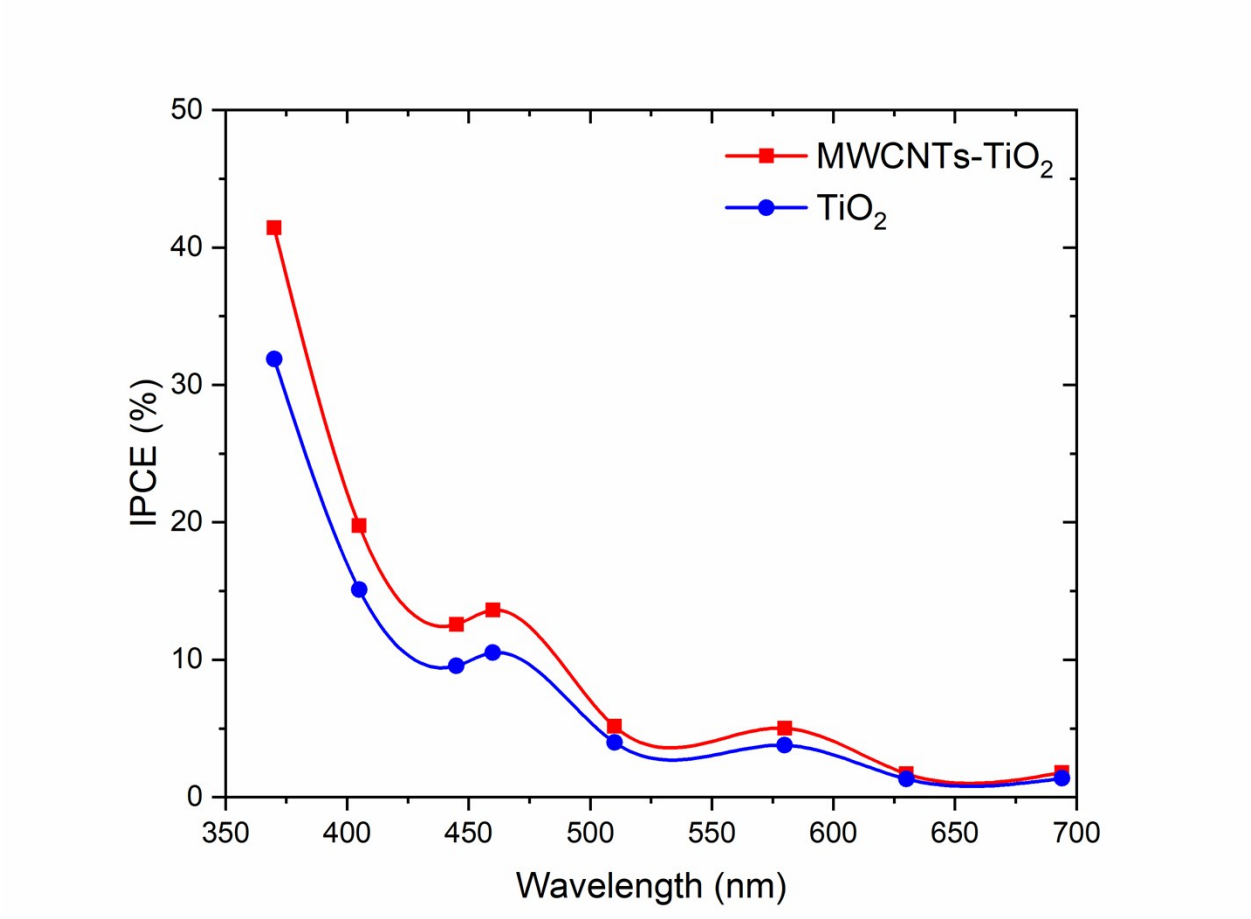

Figure 7S. Incident photon-to-current efficiency (IPCE) spectra of PEC devices based on T/Q-MWCNTs (0.015 wt.%) hybrid (red line) and T/Q bare (blue line) photoanodes measured at 1.0 V vs RHE under one sun illumination (AM 1.5 G, 100 mW.cm^{-2}).

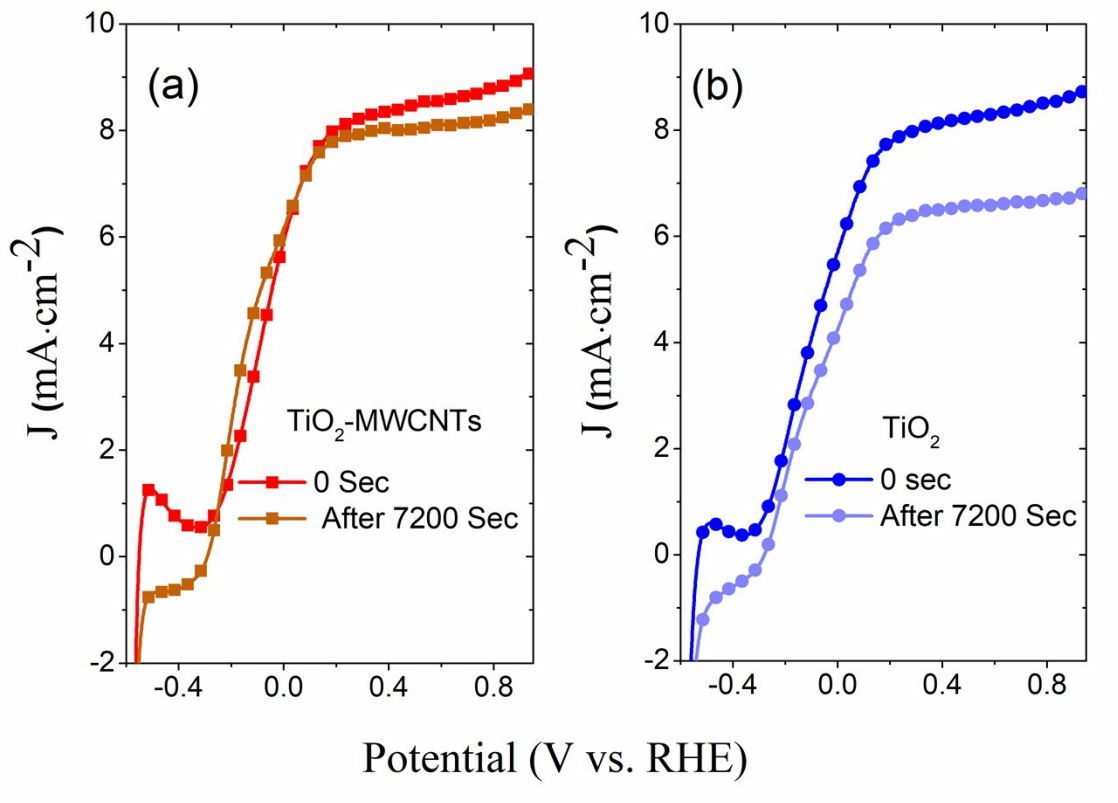

Figure 8S. Comparison of the photocurrent density versus bias potential (versus RHE) of PEC systems under one sun illumination (AM 1.5 G, 100 mW.cm^{-2}) based on: (a) TiO_2/QDs-MWCNTs hybrid fresh (red square) and after 7200 s (dark red square); (b) TiO_2/QDs fresh (blue circle) and after 7200 s (light blue circle).

Table S3. Comparison of photocurrent density of PEC devices based on colloidal core/thick-shell QDs sensitized wide band gap semiconductors of this work and reported in the literature.

Photoanode structure	**QDs shape**	**Saturated current density (mA.cm^{-2})**	**Ref.**
CdSe/($CdSe_xS_{1-x}$)/(CdS) QDs-TiO_2-MWCNTs	Spherical	15.9	This work
CdSe/$CdSe_xS_{1-x}$/CdS QDs-TiO_2	Pyramidal	12.0	4
CdSe/$Pb_xCd_{1-x}S$/CdS QDs- TiO_2	Spherical	10.2	5
CdSe/CdS QDs-TiO_2	Spherical	10.0	6

CuInSe/CuInS QDs-TiO_2	Spherical	3.1	7
CISeS/CdSeS/CdS QDs-TiO_2	Pyramidal	5.5	8
PbS/CdS QDs-TiO_2	Spherical	5.3	9

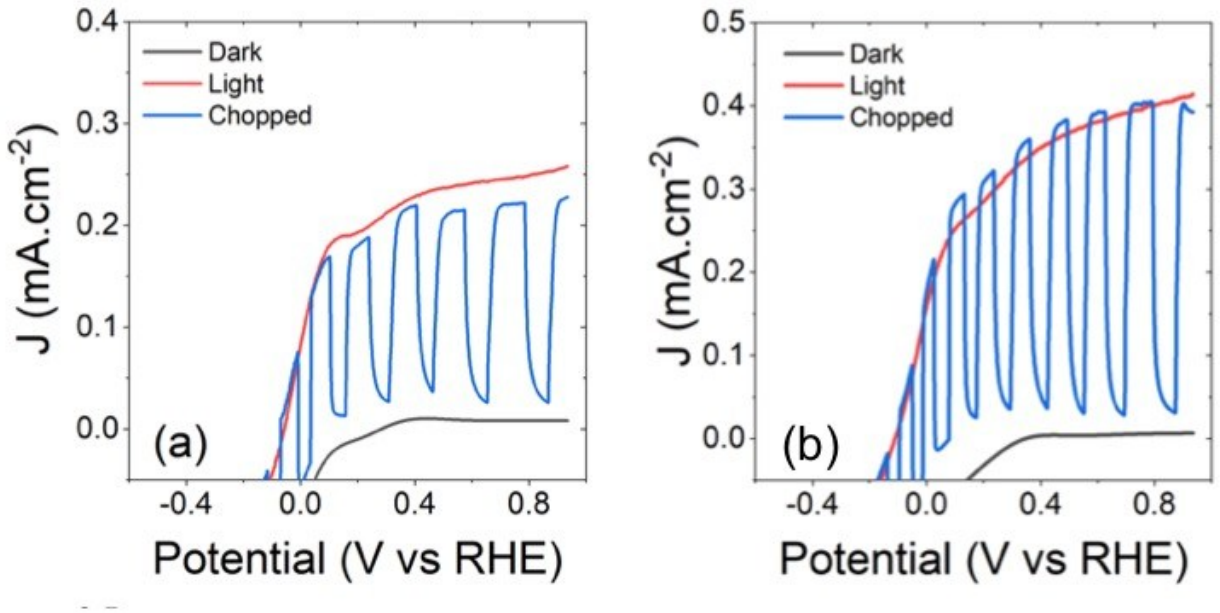

Figure 9S. Photocurrent density-potential curves of PEC devices under dark, continuous and chopped illumination (AM 1.5 G, 100 $mW.cm^{-2}$): (a) TiO_2 anode; (b) TiO_2-MWCNTs hybrid with 0.015 wt% concentration of MWCNTs.

Literature comparison of the performance of PEC devices based on TiO_2 with TiO_2-MWCNTs.

To compare the performance of PEC devices based on TiO_2 for H_2 evaluation reported in the literature with the PEC devices based on bare TiO_2 and hybrid TiO_2-MWCNTs mesoporous film prepared in this work, a series of PEC devices were fabricated by using bare TiO_2 and hybrid mesoporous film without colloidal heterostructured QDs sensitization. A systematic comparison of photocurrent density of PEC devices based on bare TiO_2 and hybrid TiO_2-MWCNTs mesoporous film (reported in this work) and PEC device based on TiO_2 (reported in the literature), calculated from current density-voltage curves under one sun illumination irradiation (AM 1.5 G, 100 mW cm^{-2}) is reported in Table S2. The photocurrent density of PEC device based on hybrid TiO_2-MWCNTs (0.015 wt.%) is 0.44 $mA.cm^{-2}$ at 1.0 V vs RHE, which is ~70% higher than the PEC device based on bare TiO_2 mesoporous photoanode (see Figure 9 S). Similarly, Morais et al. reported photocurrent density of 0.11 $mA.cm^{-2}$ at 1.23 V vs RHE under one sun illumination irradiation (AM 1.5 G, 100 mW cm^{-2}), which is further boosted to 0.20 $mA.cm^{-2}$ at 1.23 V by introducing

reduced graphene oxide (0.1 wt%) in TiO_2[10]. Furthermore, due to better electron transport properties of nanowires than nanoparticles, Hwang et al.[11] fabricated PEC devices by using rutile TiO_2 nanowires and obtained the photocurrent density of 0.73 $mA.cm^{-2}$ at 1.5 V vs RHE. This photocurrent density is significantly enhanced to 1.1 $mA.cm^{-2}$ at 1.5 V vs RHE with atomic layer deposition (ALD) of epitaxial rutile TiO_2 shell. Also, Kang et al.[12] reported the photocurrent density of 0.19 $mA.cm^{-2}$ at 1.23 V vs RHE for PEC device based on TiO_2 nanotube arrays and further boosted to 0.73 $mA.cm^{-2}$ at 1.23 V V vs RHE by reducing he TiO_2 nanotube arrays with $NaBH_4$.

Table S4. Comparison of performance of PEC devices based on TiO_2-MWCNTs in this work and PEC based on TiO_2 reported in the literature.

Photoanode structure	**Electrolyte**	**J_{sc} (mA.cm^{-2}) @ V vs RHE**	***Ref.***
TiO_2	Aqueous 0.25 M Na_2S and 0.35 M Na_2SO_3 (pH~13)	0.26 $mA.cm^{-2}$ at 1.0 V	This work
TiO_2-MWCNTs (0.015 wt%)		0.44 $mA.cm^{-2}$ at 1.0 V	
pristine TiO_2	Aqueous H_2SO_4 (0.5 mol L^{-1})	0.11 $mA.cm^{-2}$ at 1.23 V	10
Rutile TiO_2 nanowires	Aqueous 1 M NaOH	0.73 $mA.cm^{-2}$ at 1.5 V	11
TiO_2 nanotube arrays	Aqueous 1 M NaOH (pH=13.9)	0.19 $mA.cm^{-2}$ at 1.23 V	12

Reference:

1. B.O. Dabbousi, J. Rodriguez-Viejo, F.V. Mikulec, J.R. Heine, H. Mattoussi, R. Ober, K.F. Jensen and M.G. Bawendi, *J. Phys. Chem. B* 1997, **101**, 9463–9475.

2. Y. Ghosh, B. D. Mangum, J. L. Casson, D. J. Williams and H. Htoon, J. A. Hollingsworth, *J. Am. Chem. Soc,* 2012, **134,** 9634–9643.

3. (a) K. T. Dembele, G. S. Selopal, C. Soldano, R. Nechache, J. C. Rimada, I. Concina, G. Sberveglieri, F. Rosei and A. Vomiero, *J. Phys. Chem. C,* 2013, **117,** 14510–14517; (b) M. Mohammadnezhad, G. S. Selopal, Z. M. Wang, B. Stansfield and F. Rosei, *ChemPlusChem*. 2018, **83**, 682–690.

4. H. Zhao, G. Liu, F. Vidal, Y. Wang and A. Vomiero, *Nano Energy*, 2018, **53**, 116-124.

5. R. Adhikari, K. Basu, Y. Zhoua, F. Vetrone, D. Ma, S. Sun, F. Vidala, H. Zhao and F. Rosei, *J. Mater. Chem. A*, 2018, **6**, 6822-6829.

6. R. Adhikari, L. Jin, F. Navarro-Pardo, D. Benetti, B. AlOtaibi, S. Vanka, H. Zhao, Z. Mi, A. Vomiero and F. Rosei, *Nano Energ*, 2016, **27**, 265-276.
7. X. Tong, X.-T. Kong, Y. Zhou, F. Navarro-Pardo, G. S. Selopal, S. Sun, A. O. Govorov, H. Zhao, Z. M. Wang and F. Rosei, *Advanced Energy Materials*, 2018, **8**, 1701432.
8. X. Tong, X.-T. Kong, C. Wang, Y. Zhou, F. Navarro-Pardo, D. Barba, D. Ma, S. Sun, A. O. Govorov, H. Zhao, Z. M. Wang and F. Rosei, Advanced Science, 2018, **5**, 1800656.
9. L. Jin, G. Sirigu, X. Tong, A. Camellini, A. Parisini, G. Nicotra, C. Spinella, H. Zhao, S. Sun, V. Morandi, M. Zavelani-Rossi, F. Rosei and A. Vomiero, *Nano Energy*, 2016, **30**, 531.
10. A. Morais, C. Longo, J. R. Araujo, M. Barroso, J. R. Durrant and A. F. Nogueira, *Phys. Chem. Chem. Phys.*, 2016, **18**, 2608–2616.
11. Y. J. Hwang, C. Hahn, B. Liu and P. Yang, *ACS Nano*, 2012, **6**, 5060-5069.
12. Q. Kang, J. Cao, Y. Zhang, L. Liu, H. Xu and J. Ye, *J. Mater. Chem. A,* 2013, **1**, 5766–5774.